ChemComm

Accepted Manuscript

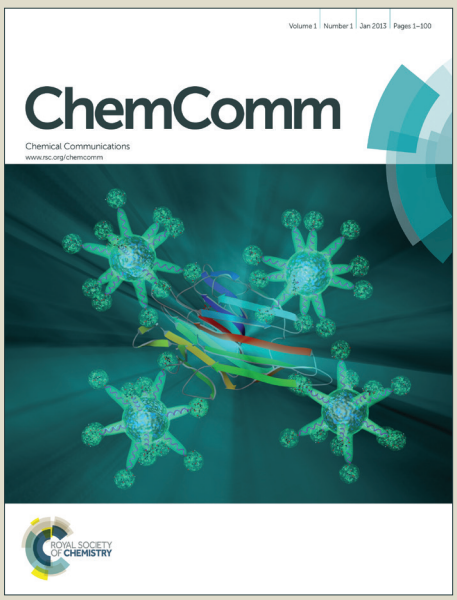

ROYAL SOCIETY OF CHEMISTRY

www.rsc.org/chemcomm

Journal Name

RSCPublishing

COMMUNICATION

Spiropyran-based X-ray sensitive fiber

Cite this: DOI: 10.1039/x0xx00000x

Kenji Kinashi [a]*, Yurika Miyamae [a], Ryotaro Nakamura [a], Wataru Sakai [a], Naoto Tsutsumi [a], Hideki Yamane [b], Gaku Hatsukano [b], Makoto Ozaki [c], Kazuya Jimbo [d], Takahiro Okabe [d]

Received 00th January 2012,
Accepted 00th January 2012

DOI: 10.1039/x0xx00000x

www.rsc.org/

This study attempted to visualize reversibly X-ray radiation by using poly-(L-lactic acid) (PLLA) composite fiber with an average diameter of 150 μm. The fiber contains photostimulable phosphor (PSP) BaFCl:Eu^{2+} particles that are subsequently dyed with the photochromic spiropyran dye 1,3,3-trimethylindolino-6'-nitrobenzopyrylospiran) (6-nitro BIPS).

Radiation protection and detection are important because of the extensive use of high-energy radiation sources in industry, medical services, scientific instruments, and nuclear power plants. In particular, addressing the unitary management of personal exposure to radiation that workers can receive while working in nuclear-related facilities is crucial. If workers can recognize their own radiation dosage early in the form of color changes to their gloves or boots, then they can avoid danger before carrying out a particular operation. Numerous studies that focus on visualization properties for X-rays or γ-rays radiation by using organic color formers have been conducted in the last decade.[1] Spiropyrans are photochromic compounds, which have attracted much interest with respect to both the fundamental elucidation of photochemical reactions and their potential application to optical memory and photo-optical switching devices.[2] In addition, spiropyrans had been basically expected to be applied to optical systems; however, another unique feature of the spiropyran has since been detected, and now they are expected to be used as sensing systems for environmental stimuli[3], such as for temperature[4], pH[5], solvent polarity[6], redox potential[7], metal ions[8], gas[9], and mechanical force[10]. X-ray storage phosphors absorb X-rays and convert the absorbed energy efficiently into ultraviolet (UV) or visible emission. Europium doped barium fluorohalides BaFX:Eu^{2+} (X = Br, Cl) have a number of favorable properties that make them suitable for use as X-ray storage phosphors in detection systems developed for two-dimensional X-ray imaging in the fields of radiography and crystallography.[11]

Quite recently, we discovered that a spiropyran-based composite film with ultraviolet-emitting X-ray storage phosphor has the characteristic of indirectly detecting high-energy synchrotron radiation.[12] The reported paper implied that the spiropyrans can provide a new, highly sensitive radioactive ray indicator that applies X-ray storage phosphors based on an operation principle that is different from a conventional X-ray sensor by improving material, composition, fashion.

The study reported herein notes a fibrous structure with high surface area to visualize radioactive rays from various angles, and is undertaken to visualize reversibly X-ray radiation by using a poly-(L-lactic acid) (PLLA) composite fiber containing photostimulable phosphor (PSP) BaFCl:Eu^{2+} particles that are prepared and then dyed with the photochromic spiropyran dye 1,3,3-trimethylindolino-6'-nitrobenzopyrylospiran) (6-nitro BIPS).

A spiropyran dye, 1',3',3'-trimethyl-6-nitrospiro[1(2*H*)-benzopyran-2,2'-indoline] (or 1,3,3-trimethylindolino-6'-nitrobenzopyrylospiran) (6-nitro BIPS) was used as the UV light-sensitive photoacceptor, and BaFCl:Eu^{2+} was used as the UV-radiation source. All solvents (tetrachloroethylene, hexane, cyclohexane, acetone, and ethyl acetate) and the 6-nitro BIPS were purchased from Tokyo Kasei Co. The BaFCl:Eu^{2+} powder was supplied from Nemoto Lumi Materials Co, and it was ground into fine particles with a lattice strain of 1% or less and then used as an ultraviolet-emitting phosphor. Poly-(L-lactic acid) (PLLA) pellets were supplied by Toyota Co. Ltd. These pellets were pre-dried at 45°C for 5 h to remove any absorbed water, thus preventing hydrolysis during the kneading and extrusion processes. The PLLA pellets (70 g) and BaFCl:Eu^{2+} powder (30 g) were premixed and fed to a twin screw extruder (Labo Plastomill μ, Toyoseki Co.), and the kneading and extrusion temperatures were both set to 195 °C on the basis of the melting temperature of PLLA. The mixed molten material was extruded into a cylindrical shape about 400 μm in diameter. The composite fibers were prepared by a melt-spinning process using a fiber making apparatus and a winding apparatus (TS. 36Z NO.83033, Torii Winding Machine Co.). After the melt-spinning process, the obtained composite fibers were immersed in a 6-nitiro BIPS solution at a concentration of 0.03 M at 40 °C for 24 h, and then washed with the same solvent.

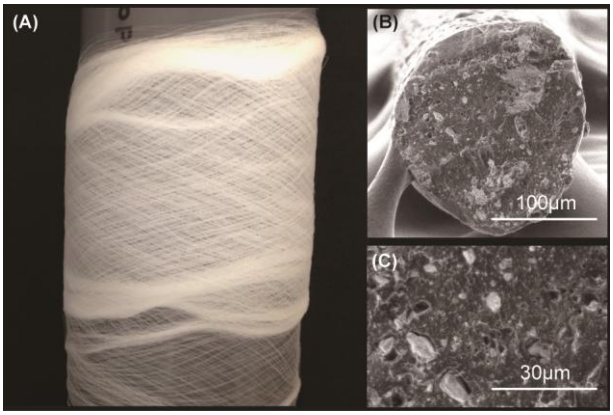

Figure 1 (A) PLLA/BaFCl:Eu^{2+} composite fiber. Aspect of the PLLA/BaFCl:Eu^{2+} composite fibers. (B,C) SEM images of the PLLA/BaFCl:Eu^{2+} composite fiber, PLLA70%/BaFCl:Eu^{2+}30%.

A cross-section image of the composite fiber was measured using a scanning electron microscope (SEM) (Hitachi S-3000). An X-ray diffractometer (Rigaku ZSX Primus II, Japan) with Cu Ka monochromated X-rays that was operated at 50 kV and 48 mA was used to produce X-radiation (0.154 nm). An X-ray excited optical luminescence spectrum of BaFCl:Eu^{2+}, which was generated with X-radiation, was guided by a photonic multi-channel analyzer (Ocean Optics Co., USB4000) through fused silica fiber (Ocean Optics Co., P400-2-UV-VIS). The UV-visible absorption spectrum was recorded with a spectrophotometer (Perkin-Elmer Co., Lambda 1050UV/Vis/NIR). The tensile test was carried out under a test speed of 20 mm/min using a tensile testing machine (STA-1150, Orientec Co.). All measurements were carried out at room temperature. The lab color space was analyzed with Photoshop software.

BaFCl:Eu^{2+}-filled polylactic acid (PLLA) composite pellets are prepared by kneading and extrusion processes. The composite fiber consists of PLLA and BaFCl:Eu^{2+} at a mixing ratio of 70/30 wt%. The kneading and extrusion processes led to a uniform distribution of the BaFCl:Eu^{2+} particles in the PLLA. The aspect of the composite fiber that was prepared by melt-spinning is shown in **Figure 1**. The scanning electron micrographs (SEM) of the cross-section of the composite fiber show that the diameter length is 150 μm, and the BaFCl:Eu^{2+} particles are observed to have a distribution of particle sizes with lengths ranging from below 1 μm up to a maximum of 10 μm. The denier of the composite fibers is estimated to be 610 denier according to the analysis of the SEM image. The SEM analysis shows that the particles have a wide size distribution and that most of these particles have a non-unity aspect ratio even though they are neither rod-shaped nor fiber-like. These particles were also observed to have an irregular and rough surface. A tensile modulus of the composite fibers was measured to be 2333.2 MPa, and their composite fibers averagely showed a modulus of elasticity higher than that of the PLLA fiber by 155% after kneading the BaFCl:Eu^{2+}.

After the melt-spinning process, the composite fiber was dyed with 6-nitiro BIPS photochromic dye in tetrachloroethylene at 40 °C for 24 h to ensure deep dyeing. **Figure 2A** shows the photochromic reaction of the 6-nitro BIPS irradiated by 365-375 nm light of UV-LED (90 mW/cm^2). Under the UV light, the color of a yarn made by twining the 6-nitro BIPS dyed composite fibers changed from colorless to purple, which is attributed to the fact that the spirocarbon–oxygen (C–O) bond in the closed form of a colorless spiropyran (SP-form) is cleaved, and the subsequent isomerization leads to the open form of a colored isomer, referred to as open photomerocyanine (PMC-form). **Figure 2B** and **2C** shows the dynamic behavior of the colored yarn under daylight at room temperature. The monitored reflectance was defined by the centered reflectance peak of the PMC-form. The photochromic backward reaction curve of the reflectance corresponded well to a single exponential decay function. According to the conventional approach for evaluation of the single exponential function, the backward reaction time constant was estimated to be 14 min. In the case of the backward reaction in the dark condition, that time constant was estimated to be 66 min. In addition, color strength of the colored yarn is also presented as total *K/S* values of the K/S values of the respective wavelengths. The *K/S* values were calculated using the Kubelka-Munk Equation (1):

$$K/S = (1-R)^2/2R \qquad (1)$$

where *R* is the observed reflectance, *K* is the absorption coefficient and *S* is the light scattering coefficient. As a result, the same tendency was confirmed when compared with the reflectance curve of the colored yarn, and the color strength (*K/S*) of the colored yarn is estimated to be 37. Aspects of the yarn made by twining the 6-nitro BIPS dyed composite fibers before and after UV irradiation are shown in **Figure 2D** and **2E**. After stopping the UV light irradiation, the absorption band of the PMC-form gradually decreased for approximately a few minutes at an ambient temperature; however, the decay time of the colored PMC-form unfolded over the course of an entire day at ambient temperatures. The reason for the prolonged decay time of the colored PMC-form is possibly due to other additives, such as surfactant[13] or silica[14], as well as polar environment[15], based on the studies we reported previously. Thus, when a UV protection is applied on the yarn, the colored PMC-form is returned to the colorless SP-form only by a heat treatment, which means that erasure of the record or reuse of the material will be possible. An another important property of the dyed composite fiber is that its color changes can be uniformly confirmed as a whole, which indicates that the 6-nitro BIPS penetrated to the depth of the composite fiber, because the organic solvent tetrachloroethylene plays a role of a carrier to help the 6-nitro BIPS penetrate deeply. The result indicates that the presence of tetrachloroethylene as a carrier contributed the deep dyeing, because the solubility of the 6-nitiro BIPS for tetrachloroethylene is high. Assuming that the process of dye diffusion into the composite fiber is followed by an interfacial diffusion, the dyeing process should be governed by partition coefficient log*P*, which is calculated in equation (2).

$$\log P = \log(C_{Fiber}/C_{Dyebath}) \qquad (2)$$

At constant temperature, the partition coefficient log*P*, i.e., the ratio of the concentration of dye dissolved in the fiber (dye uptake) (C_{Fiber}, mol kg^{-1}) versus the dye remaining in the dyebath (C_{Bath}) at equilibrium, is constant. The dye uptake C_{Fiber} is determined by measuring the absorbance of the diluted dyebath at the wavelength of the peak top (331 nm) of the SP-form. The concentration of dye

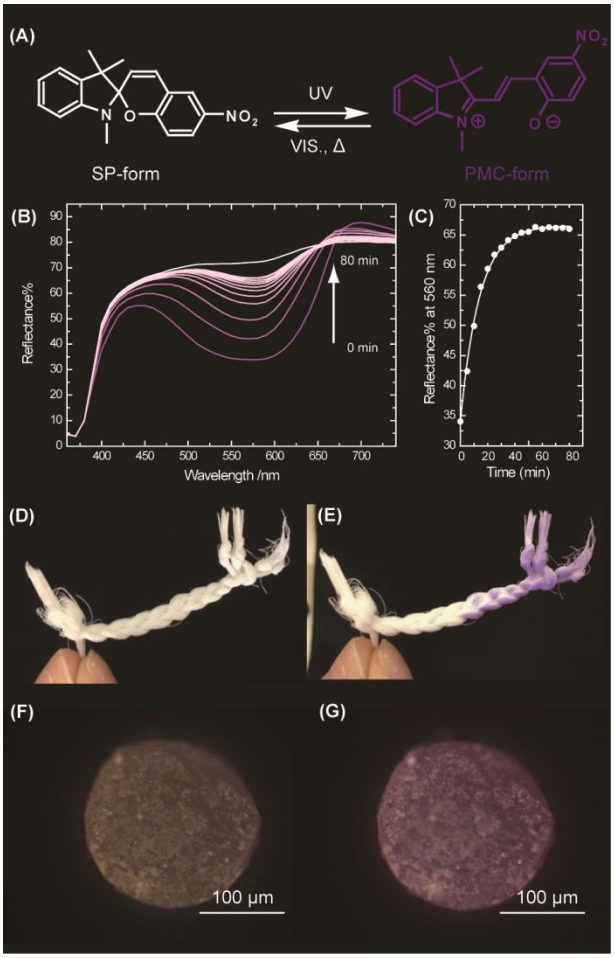

Figure 2 (A) Reversible photoisomerization of the 6-nitro BIPS. Photograph showing the yarn made by twining the 6-nitro BIPS dyed composite fibers before (B) and after (C) UV irradiation, and CCD images of a cross-section of the 6-nitro BIPS dyed composite fiber before (D) and after (E) UV irradiation.

uptake C_{Fiber} is estimated from absorbances of the dyebath before and after dyeing, which is calculated using Equation (3):

$$C_{Fiber} = \left[\frac{(A_0 - A_1)V}{\varepsilon \ell} / W_{Fiber} \right] \quad (3),$$

where A_0 and A_1 are respectively the absorbance of the dyebath before and after dyeing, V is the volume of the dyebath, ε is the molar extinction coefficient of the SP-form at the peak top (331 nm), l is the path length of a quartz cell, and W_{Fiber} is the weight of the fiber. The calculation shows that the partition coefficient log$P$ of the composite fiber that contains 6-nitro BIPS in tetrachloroethylene has a value of 1.18 L kg^{-1} during the dyeing process. This result indicates that the high solubility contributes to the dye distribution throughout the composite fiber as it carries the 6-nitro BIPS deep into the fiber, as shown in **Figure 2F** and **2G**; however, the high solubility conversely restricts high concentration dyeing because of the low partition coefficient. Partition coefficients tend to show lower values for a tetrachloroethylene dyebath than those in an aqueous system because of the former's lower solubility. Accordingly, the diffusion coefficient might be improvable with water, a mixed solvent, or supercritical carbon dioxide in the future. In particular, it is expected

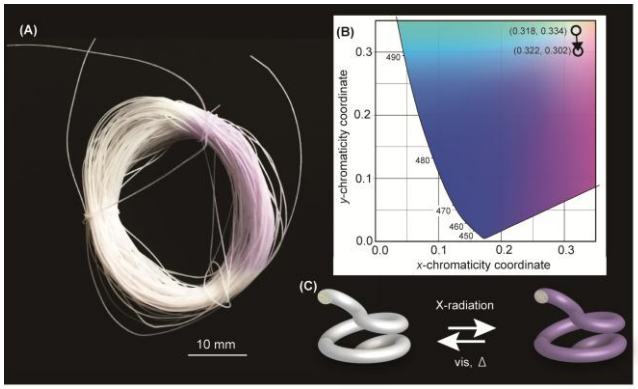

Figure 3 (A) Photograph showing the 6-nitro BIPS composite fibers before (left side) and after (right side) X-ray exposure. (B) Color shift in the CIE1931 chromaticity diagram at the maximum brightness; color coordinates of the 6-nitro BIPS dyed composite fiber are shown as open circles in (B). (C) The schematic representation of X-ray visualization using the 6-nitro BIPS dyed composite fiber.

that use of supercritical carbon dioxide for disperse dye will enhance the partition coefficient more than 10-100 times, because its solubility remains lower than that of the tetrachloroethylene system, and yet its partition coefficient becomes high.[16]

The BaFCl:Eu^{2+} crystal is one of the PSPs that emit a near-ultraviolet light upon irradiation with X-rays, and β-rays at room temperature. The BaFCl:Eu^{2+} powder displays a strong photoluminescence centered at 381 nm, which is attributed to an electronic transition from the $4f^6 5d^1$ (^2e_g) state of Eu^{2+} to the $4f^7$ ($^8S_{7/2}$) ground state upon irradiation with X-rays of 0.154 nm at room temperature.[17] Accordingly, the strong photoluminescence of near-ultraviolet light at 381 nm can overlap with the region in which the photoisomerization of SP-to-PMC occurs.

A practical application of X-ray visualization using the dyed composite fiber is shown in **Figure 3A**. The photograph exhibits a change in color of the dyed composite fiber before and after X-ray exposure at room temperature. The left side of the photograph shows the appearance of the dyed composite fibers before X-ray exposure. There, the dyed composite fiber is a white color that is derived from a combination of the colorless SP-form and the BaFCl:Eu^{2+} powders. Upon X-ray exposure for 73 s (a dose corresponding to 7.41 Gy; Fig. S1, ESI†), the color of the dyed composite fiber reversibly changes from white to pale purple. The color change can be explained in detail by the color difference Commission Internationale de l'Eclairage (CIE) chromaticity diagram. **Figure 3B** shows that the CIE chromaticity coordinates (x, y) are found to be from (0.318, 0.334) to (0.322, 0.302). For the respective colors, the CIE L*a*b* are as follows: L^* is 83.76 to 52.12; a^* is -1.43 to 12.39; and b^* is 0.92 to 33.51; thus, the magnitude of total color difference ΔE^*_{ab} is calculated to be +45.28. ΔE^*_{ab} according to Equation (4):

$$\Delta E^*_{ab} = \left[(\Delta L^*)^2 + (\Delta a^*)^2 + (\Delta b^*)^2 \right]^{1/2} \quad (4)$$

where ΔL^* is the lightness difference, Δa^* the red/green difference, and Δb^* the yellow/blue difference. The ΔE^*_{ab} value shows +48.76, which fulfils the requirement value of 10 or higher (people can

recognize changes in color of a magnitude of 10 or higher). By further improving the dye uptake and partition coefficient, we will provide an excellent composite fiber as a yarn of a radioactive ray indicator that can readily detect radioactive rays with high sensitivity and that permits quantitative measurement of the degree of irradiation of the detected rays. The schematic representation of X-ray visualization using the dyed composite fiber is depicted in **Figure 3C**.

In conclusion, the 6-nitro BIPS-dyed composite fiber easily visualizes X-rays. The reversible visualization characteristics for X-rays that can be achieved using the 6-nitro BIPS dyed composite fiber can be utilized as an alternative product for the EBT Gafchromic film. Furthermore, the visualization property for radioactive rays, including X-rays, will help to address a serious situation in Japan—nuclear plant workers face the risk of excessive radiation exposure. If they could clearly see their radiation dose in the form of color changes in their gloves or boots, then they would be able to avoid unexpectedly dangerous situations.

This work was financially supported by JSPS Grant-in-Aid for Young Scientists (B) 26820305, and NISSHA PRINTING CO., LTD.

Notes and references

1 (a) S. Irie and M. Irie, Chem. Lett., 2006, 35, 1434; (b) T. Tachikawa, K. Akagi and S. Tokita, J. Photopolym. Sci. Technol., 2005, 18, 121; (c) H. Itoi, Y. Sekine, M. Sekiguchi and T. Tachikawa, Chem. Lett., 2009, 38, 1002; (d) K. Kinashi, Y. Miyashita, K. Ishida and Y. Ueda, J. Phys. Org. Chem., 2012, 25, 427; e) M. -S. Wang, C. Yang, G.-E. Wang, G. Xu, X.-Y. Lv, Z.-N. Xu, R.-G. Lin, L.-Z. Cai, G.-C. Guo, Angew. Chem. Int. Ed. 2012, 51, 3432.

2 (a) F. M. Raymo, Adv. Mater. 2002, 14, 401; (b) 2 S. Giordani, M. A. Cejas and F. M. Raymo, Tetrahedron 2004, 60, 10973; (c) F. M. Raymo and M. Tomasulo, Chem. Soc. Rev., 2005, 34, 327; (d) G. Berkovic, V. Krongauz and V. Weiss, Chem. Rev., 2000, 100, 1741.

3 R. Klajn, Chem. Soc. Rev., 2014, 43, 148.

4 V. I. Minkin, Chem. Rev., 2004, 104, 2751.

5 F. M. Raymo and S. Giordani, J. Am. Chem. Soc., 2001, 123, 4651.

6 R. Rosario, D. Gust, M. Hayes, F. Jahnke, J. Springer and A. A. Garcia, Langmuir, 2002, 18, 8062.

7 K. Wagner, R. Byrne, M. Zanoni, S. Gambhir, L. Dennany, R. Breukers, M. Higgins, P. Wagner, D. Diamond, G. G. Wallace and D. L. Officer, J. Am. Chem. Soc., 2011, 133, 5453.

8 D. A. Parthenopoulos and P. M. Rentzepis, Science, 1989, 245, 843.

9 Y. -S. Nam, I. Yoo, O. Yarimaga, I. S. Park, D. -H. Park, S. Song, J. -M. Kim and C. W. Lee, Chem. Commun., 2014, 50, 4251.

10 D. S. Tipikin, Russ. J. Phys. Chem., 2001, 75, 1720.

11 (a) M. Sonoda, M. Takano, J. Miyahara and H. Kato, Radiology, 1983, 148, 833; (b) S. Schweizer, Phys. Stat. Solidi A, 2000, 187(2), 335.

12 K. Kinashi, K. Jimbo, T. Okabe, S. Sasaki and H. Masunaga, Int. J. Photoenergy, 2014, 2014, 236382.

13 K. Kinashi, T. Horiguchi, K. Tsutsui, K. Ishida and Y. Ueda, J. Photochem. Photobiol. A: Chem., 2010, 213, 189.

14 K. Kinashi, S. Nakamura, Y. Ono, K. Ishida and Y. Ueda, J. Photochem. Photobiol. A: Chem., 2010, 213, 136.

15 K. Kinashi, Y. Harada and Y. Ueda, Thin Solid Films, 2008, 516, 2532.

16 (a) S. K. Liao, Indian J. Fibre Text. 2005, 30, 324; (b) T. Hori, Kobunshi Ronbunshu (in Japanese), 55 (12) (2006).

17 (a) W. Chen, N. Kristianpoller, A. Shmilevich, D. Weiss, R. Chen and M. Su, J. Phys. Chem. B, 2005, 109, 11505; (b) W. Chen, Q. Song and M. Su, J. Appl. Phys., 1997, 81(7), 1.

[a] *Department of Macromolecular Science and Engineering, Graduate School of Science and Technology, Kyoto Institute of Technology, Matsugasaki, Sakyo, Kyoto 606-8585, Japan. E-mail: kinashi@kit.ac.jp*

[b] *Department of Biobased Materials Science, Graduate School of Science and Technology, Kyoto Institute of Technology, Matsugasaki, Sakyo, Kyoto 606-8585, Japan*

[c] *Advanced Technology Center, Kyoto Institute of Technology, Matsugasaki, Sakyo, Kyoto 606-8585, Japan*

[d] *NISSHA PRINTING CO.,LTD, 3 Mibu, Hanai,Nakagyo, Kyoto 604-8551 Japan*

† Electronic Supplementary Information (ESI) available: [details of any supplementary information available should be included here]. See DOI: 10.1039/c000000x/